Quarkyonic stars with isospin-flavor asymmetry

Jérôme Margueron, Hubert Hansen, P. Proust, G. Chanfray

Quarkyonic stars with isospin-flavor asymmetry

Jérôme Margueron,[1] Hubert Hansen,[1] Paul Proust,[1] and Guy Chanfray[1]

[1] *Univ Lyon, Univ Claude Bernard Lyon 1, CNRS,*
IP2I Lyon / IN2P3, UMR 5822, F-69622, Villeurbanne, France
(Dated: March 19, 2021)

We suggest an extension to isospin asymmetric matter of the quarkyonic model from McLerran and Reddy [1]. This extension allows us to construct the β-equilibrium between quarks, nucleons and leptons. The concept of the quarkyonic matter originates from the large number of color limit for which nucleons are the correct degrees of freedom near the Fermi surface – reflecting the confining forces – while deep inside the Fermi sea quarks naturally appear. In isospin asymmetric matter, we suggest that this new concept can be implemented within a global isoscalar relation between the shell gaps differentiating the nucleon and the quark sectors. In addition, we impose the conservation of the isospin-flavor asymmetry in the nucleon and the quark phases. Within this model, several quarkyonic stars are constructed on top of the SLy4 model for the nucleon sector, producing a bump in the sound speed, which implies that quarkyonic stars are systematically bigger and have a larger maximum mass than the associated neutron stars. They also predict lower proton fraction at β-equilibrium, which potentially quenches fast cooling in massive compact stars.

Recent observations of neutron stars (NS), such as radio and x-ray astronomy, or the detection of gravitational wave (GW) detection, have provided the tightest constraints on the dense matter equation of state (EoS) to date [2–4]. These constraints can be classified into different groups: the first one refers to the highest NS masses ever observed [5–10], estimated to be about $2M_\odot$, with some indications that the maximum mass could eventually be larger [9, 10]. The second group assembles constraints from binary NS (BNS) GW detection in the inspiral phase, from which the tidal deformability is estimated [11, 12] . It includes GW170817 [4] and further detections. The third group still refers to NS mergers, more specifically to the analysis of the electromagnetic (EM) counterpart, see Ref. [13] for instance and refs. therein. The fourth group matters with x-ray observations, such as thermal emission from qLMXB [14–16], x-ray burst and photospheric expansion [6, 17], as well as x-ray emission from hot-spots at the surface of some NS (NICER) [18].

The analysis of these new data requires to set-up generic models for the EoS, with various levels of agnosticity to model assumptions, such as the isospin asymmetry for instance, or the interaction prerequisites, inducing possible spurious constraints among observables. As an illustration, the nuclear meta-model [19] can be used to explore predictions compatible with the assumption that matter is uniquely composed of nucleons (and of course leptons). It can also be employed for the description of phase transitions. This is the purpose of this paper: exploring the nucleon-quark phase transition in compact stars where this transition is described with the quarkyonic model [1].

The quarkyonic model for dense matter proposed in Ref. [20] (and recently applied to neutron stars in Ref. [1]) is one of them. It is an interesting candidate to bridge the gap in describing quark matter and nuclear matter at the phase transition [21]. The quarkyonic model is not properly a microscopic model since it is not based

on the QCD Lagrangian or an effective version of it, but it implements some features from in the large number of color (N_c) limit of QCD [20] with few parameters. New configurations at high and low temperature limit of the holographic Witten-Sakai-Sugimoto model has recently been interpreted as holographic realizations of quarkyonic matter in isospin symmetric matter, based on a quark Fermi sea enclosed by a baryonic layer on momentum space [22]. In the real-world where $N_c = 3$, it possibly approximates the actual ground state of dense matter and the confrontation of its predictions to the data can be used to determine the model parameters. These parameters happen to be physical and thus meaningful: they are the quarkyonic scale $\Lambda_{\mathrm{Qyc}} \approx 250 - 300$ MeV, which is comparable to the QCD scale Λ_{QCD}, and κ_{Qyc} which controls the saturation of the nucleonic shell [20].

The interesting feature of the quarkyonic model is that it suggests a cross-over between the hadron phase and the quark one, at variance with other approaches such as the ones based on Maxwell/Gibbs construction. Note that cross-over are also suggested from Cooper pairing in the hadron and in the quark phases. The quarkyonic cross-over is thus another example of such features. It however disregards one of the essential prediction of QCD, namely the restoration – as the density increases – of chiral symmetry which is spontaneously broken in the QCD vacuum. Note that in the holographic approach from Ref. [22], chirally restored and chirally broken quarkyonic matter are constructed, and it was found that only chirally restored matter is energetically preferred. In widely used quark models implementing the chiral symmetry breaking, e.g. Nambu–Jona-Lasinio approach, the transition between the broken phase assimilated to the hadronic phase and the restored one assimilated to the free quark phase is however generally first order (for most parameter sets). In the future, it would be interesting to combine together in isospin asymmetric matter the phenomenology of the color gauge symmetry realized at large N_c and the chiral symmetry dynamics, both rooting into

the QCD Lagrangian.

In the cross-over region, the quarkyonic model suggests that the pressure first increases at the onset of the first quarks, while first order phase transition models usually suggest a softening of the pressure due to the increase of the degrees of freedom [23, 24]. The consequence is the large increase of the energy density, as well as a peaked sound speed at a density of about 2-3 times the saturation density of nuclear matter, $n_{\text{sat}} \approx 0.16 \, \text{fm}^{-3}$, as expected by some authors [25, 26].

These features are characteristic to the quarkyonic model – however not specific – and have motivated further investigations and applications to neutron star physics. In the original paper by McLerran and Reddy [1], the quarkyonic matter was studied in the case of isospin symmetry (symmetric matter, SM) as well as in the case of neutron matter (NM). The application to neutron star has been performed assuming it is composed only of neutrons, and u and d quarks within the ratio satisfying local charge neutrality, $k_{Fd} = 2^{1/3}k_{Fu}$ where k_{Fd} (k_{Fu}) is the d (u) quark Fermi momentum. A version of the quarkyonic model for isospin asymmetric matter, where the isospin asymmetry is controlled by the chemical equilibrium, was then suggested by Zhao and Lattimer [27]. In their model, Zhao and Lattimer have treated nucleons and quarks as independent particles for which the energy minimization imposes the equilibrium between their respective chemical potential. They found that their quarkyonic stellar model is able to satisfy observed mass and radius constraints with a wide range of model parameters. They also predict that quarkyonic matter tends to reduce the proton fraction, compared to the nucleonic case. This reduces the domain of parameter allowing the direct URCA process [28]. It was also suggested by Jeong, McLerran and Sen [29] that the hard core in the nucleon interaction could be represented by an excluded volume, which in turns can be related to the shell gap controlling the cross-over properties. In such model, the shell gap is directly controlled by the size of the hard core. Similarly to the original paper by McLerran and Reddy [1], this model also predicts the presence of a peak in the sound speed at 2-3n_{sat}. It was also extended to describe three-flavor baryon-quark mixtures, allowing the onset of strange particles [30, 31].

In this paper, we suggest another version of the quarkyonic model for isospin asymmetric matter (AM) where we investigate the analogy between the quarkyonic model and the Cooper pair formation around the Fermi energy [1]. While this analogy may appear as rather simplistic, it suggests that quarks and nucleons may be viewed as two representations of the same quasi-particle excitation, in the same way as Cooper pairs and single particles coexist in superfluids or superconductors, but in different regions of the nuclear spectrum [32]. In AM, the neutron/proton ratio in the nucleon sector and the flavor asymmetry in the quark sector are fixed by the compound nature of the nucleons, since $n : udd$ and $p : uud$. In this spirit, quarks and nucleons are not distinguished as two independent particles for which the energy minimization imposes an equilibrium relation, as suggested in the quarkyonic model of Zhao and Lattimer [27]. In addition, the β-equilibrium does not involve quark chemical potentials since only nucleons are occupying the Fermi levels. Our picture requires a new approach for the thermodynamical construction of the phase equilibrium. The cross-over, as described in the original quarkyonic model [1], is depicted by an isoscalar condition connecting the momenta of the quarks and of the nucleons, while the isospin/flavor asymmetry in the quark and the nucleon sectors is fixed. Under these two assumptions, the model we propose describes the phase transition from symmetric to neutron matter.

In our picture, there is no direct contribution of the quarks to the β-equilibrium since they do not occupy Fermi levels. The presence of quarks however influences the β-equilibrium, through their contribution to the nucleon chemical potentials. This picture breaks down in the pure quark phase, which does not occurs in the quarkyonic model since there is always a small but finite contribution of nucleons at high density. In addition the chiral symmetry generating the constituent quark mass is assumed to remain at all density, even in the dense phases where quarks become the dominant species. This is also an interesting suggestion from the quarkyonic model which goes against the usual picture of the hadron-quark phase transition based on chiral symmetry restoration. As we stated earlier, on the one hand the quarkyonic transition is driven by features of QCD relying on its gauge theory nature at large N_c, where only planar graphs survive, whereas on the other hand the transition follows the chiral symmetry restoration (property of the quark sector only) which induces a large change of the constituent masses and also of the baryon properties. In the future, a model unifying both mechanisms in isospin asymmetric matter would be an interesting theoretical development.

In this paper, we suggest an extension of the original quarkyonic model [1] for AM in Sec. I. The cold catalyzed NS EoS – at β-equilibrium – is derived in Sec. II and finally we calculate NS properties in Sec. III. We finally conclude and suggest outlook in Sec. IV.

I. QUARKYONIC MODEL IN ASYMMETRIC MATTER

The concept of quarkyonic matter has emerged in the large number of color, N_c, limit of QCD [20]. In this limit and when the nucleon density n_N is much larger than the QCD scale, $n_N \gg \Lambda_{\text{QCD}}^3$, the confining potential of QCD is dominant even though the nucleonic Fermi momentum is large, $k_{F_N} \gg \Lambda_{\text{QCD}}$. The concept of quarkyonic matter has been introduced in order to resolve this apparent paradox: the ground state of dense matter is composed of dressed quarks (with mass $\simeq M_N/3$) that are freely moving deep inside the Fermi sea, and of a shell of baryons

generated by the strong confining force, which lies close to the Fermi level [20]. Baryons occupies a momentum shell whose width is taken to be $\Delta_{\text{Qyc}} \approx \Lambda_{\text{Qyc}}$, while deepest states are occupied by quarks.

Even if matter is composed of nucleons and quarks, low energy excitations around the Fermi level involve only quasi-particles of nucleonic type. The excitation of quarks require the expense of a momentum of the order of the shell width Δ_{Qyc}. In this prospect, nucleons and quarks are not independent particles, but there are realization of matter excitations in well separated energy regions. This picture is clearly illustrated on the left panel of Fig. 1 for SM.

In SM, this picture is simple since it is sufficient to fix a condition between the nucleon and quark single particle energies $\epsilon_N(k)$ and $\epsilon_Q(k)$ to separate the deep quark states from the nucleons ones located around the Fermi level. This condition imposes that the last quark occupied state coincides with the first nucleon one [1],

$$\epsilon_N^{\text{NI}}(k_{F_N} - \Delta_{\text{Qyc}}) = N_c \epsilon_Q(k_{F_Q}) \qquad (1)$$

where k_{F_N} and k_{F_Q} are isoscalar nucleon and quark Fermi momenta. The factor N_c in Eq. (1) stands for the number of quarks forming each nucleon in its ground state. With this condition, the nucleon and quark degrees of freedom are reduced to only one free variable, that we fix to be k_{F_N}, the nucleon Fermi momentum for convenience. Note that in Eq. (1) the nucleon single particle energy is the non-interacting (NI) one, $\mathcal{E}_N^{\text{NI}}(k) = \sqrt{M_N^2 + k^2}$. This choice is performed in order to avoid unnecessary complication of the model. We further assume that chiral symmetry remains broken to set the quark mass ($M_u = M_d = M_Q$) with $M_Q \approx M_N/N_c$, as in the constituent quark model.

Finally a prescription for the thickness of Fermi layer where nucleons reside has to be taken. We adopt the same relation from the original paper [1],

$$\Delta_{\text{Qyc}} = \frac{\Lambda_{\text{Qyc}}^3}{\hbar c^3 k_{F_N}^2} + \kappa_{\text{Qyc}} \frac{\Lambda_{\text{Qyc}}}{\hbar c N_c^2}, \qquad (2)$$

with $\Lambda_{\text{Qyc}} \approx 250 - 300$ MeV and $\kappa_{\text{Qyc}} \approx 0.3$. Δ_{Qyc} defines the energy scale below which nucleons reside.

The concept of quarkyonic matter however leads to a fundamentally new way to represent the nucleon and quark densities n_N and n_Q and their associated Fermi seas. As in a superfluid, there is only one chemical potential that enters into the thermodynamic equilibrium, and which is associated to the last nucleon occupied state $\mu_N = E(N_B) - E(N_B - 1)$ where E is the total baryon energy in the ground state and N_B stands for the number of baryons which is a partition of nucleons and quarks states. By adding or removing a baryon, the entire Fermi sea is reorganized leading to a new partition between quark and nucleon states, with the condition on the number densities $n_B = n_N + n_Q$. This new concept is first applied to symmetric and neutron matter [1] and we are now suggesting an extension for AM.
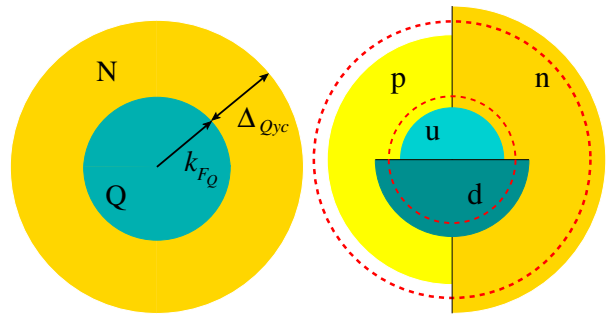

FIG. 1: Schematic views of the different Fermi seas at stake in quarkyonic matter for SM (left) and AM (right). Quarks occupy deep states inside their Fermi spheres while nucleons occupy the shells close to their Fermi levels.

A. Global isoscalar relation between nucleon and quark Fermi seas

By breaking the isospin symmetry in AM, the nucleon and quark states are replaced by four other states: neutrons, protons, as well as u and d quarks are the natural components in AM, where they are represented by their associated densities, n_n, n_p, n_u and n_d. The four Fermi seas are schematically represented in the right panel of Fig. 1. The baryon charge density controlling SM is completed in AM by the isospin asymmetry δ_N. Since there are only two charges and four particles, the concept of quarkyonic matter in asymmetric matter requires two additional relations.

At variance with SM where nucleons and quark Fermi seas could be defined by imposing a relation between their single particle energies, see Eq. (1), nothing similar can be done in AM between the four particles. The concept of quarkyonic matter suggests however that the relation between nucleons and quarks in SM, see Eq. (1), remains globally valid in AM. The nucleon and quark Fermi momenta in AM, k_{F_N} and k_{F_Q}, are represented in Fig. 1 by the red dashed circles.

Expanding the single particle energies in Eq. (1), e.g. $\mathcal{E}_Q(k) = \sqrt{M_Q^2 + k^2}$, one gets the following relation between the nucleon and quark isoscalar Fermi momenta,

$$k_{F_Q} = \frac{k_{F_N} - \Delta_{\text{Qyc}}}{N_c} \Theta(k_{F_N} - \Delta_{\text{Qyc}}). \qquad (3)$$

Note that in Eq. (3) we assumed that the nucleon shell gap Δ_{Qyc} is also an isoscalar quantity. Eq. (3) allows quark to appear as soon as $k_{F_N} - \Delta_{\text{Qyc}} > 0$ independently of the isospin asymmetry. This is supported, as we explain previously, by the idea that exciting quarks in AM requires an energy of the order of Δ_{Qyc} irrespectively of the partition of matter between neutrons and protons. Without an actual solution of QCD, this assumption is the simplest one which can be done.

The limit of NM was also explored in the original paper by McLerran and Reddy [1]. The prescription taken there imposes that one has to choose which among u and d quarks are connected to the neutron states. In addition, the value for $\Lambda_{\mathrm{Qyc}} = 300$ MeV considered in SM was changed to 380 MeV in NM. In our model, Λ_{Qyc} is taken constant, but the change of the Fermi momentum between SM and NM, see Eqs. (3) and (17), induces an effective modification of Λ_{Qyc} between SM and NM with the ratio $2^{1/3}$, which is exactly the same ratio considered by McLerran and Reddy [1]. In practice, the two approaches lead to similar results in NM. The isoscalar relation (3) presents however the advantage to describe AM and to recover the limit of SM, where the concept of the quarkyonic matter is simple.

In summary, we remark that the isoscalar Fermi momentum k_{F_N} controls both the isoscalar quark Fermi momentum k_{F_Q}, see Eq. (3), as well as the nucleon gap (3) from the prescription (2). The isoscalar nucleon and quark densities can be safely determined as,

$$n_N = \frac{2}{3\pi^2}\left[k_{F_N}^3 - (k_{F_N} - \Delta_{\mathrm{Qyc}})^3 \Theta(k_{F_N} - \Delta_{\mathrm{Qyc}})\right],\tag{4}$$

and the quark density,

$$n_Q = \frac{2}{3\pi^2}k_{F_Q}^3 \Theta(k_{F_Q}).\tag{5}$$

The total baryon density is built upon the nucleon and quark contributions as,

$$n_B = n_N + n_Q.\tag{6}$$

While the isoscalar densities n_N and n_Q can now be calculated from k_{F_N}, the connection to the densities of the four particles n, p, u and d are yet unknown. They are related to the isoscalar densities from the following relation:

$$n_N = n_n + n_p\tag{7}$$
$$n_Q = (n_d + n_u)/N_c.\tag{8}$$

In the following, we suggest that the densities n_n, n_p, n_u and n_d can be obtained in AM by imposing the isospin/flavor asymmetry in the nucleon and quark phases.

B. Isospin/flavor asymmetry

We will now determine the particle densities. In the quarkyonic model, there is a partition between nucleons and quarks which changes as the density evolves. It reveals the dynamical process converting quarks into nucleons or breaking the nucleons into their constituents, as it shall be in compound systems. A simple way to translate this symmetry into the nucleon and quark phases is to impose that the two phases conserve the isospin/flavor asymmetry. Since $n : (udd)$ and $p : (uud)$, we obtain

the following relations for the quark density in the nucleon phase, $n_u^{\mathrm{nuc}} = n_n + 2n_p$ and $n_d^{\mathrm{nuc}} = 2n_n + n_p$, which leads to the following simple connection between the isospin asymmetry parameter $\delta_N = (n_n - n_p)/n_N$ in the nucleon phase and the flavor asymmetry parameter $\delta_Q = (n_d - n_u)/(n_d + n_u)$ in the quark phase:

$$\delta_N = N_c \delta_Q.\tag{9}$$

From SM to NM, δ_N goes from 0 to 1, while δ_Q goes from 0 to $1/N_c$. The dynamics of the phase transition thus imposes that the u and d flavor ratio reflects the isospin asymmetry of the nucleon phase.

As a side note, we are aware that the isospin/flavor asymmetry relation (9) can possibly be violated by the two phases if the energy minimization is injected. Such a refinement of the quarkyonic model is indeed very interesting but it complexifies the quarkyonic approach, which nice feature remains in its simplicity. Further extensions of the present model will be explored in the future, especially to analyze their role in the predictions presented here.

Knowing δ_N and k_{F_N} – which fixes n_N and n_Q – one can deduce all particle densities as

$$n_n = \frac{1+\delta_N}{2}n_N \equiv x_n n_N,\tag{10}$$

$$n_p = \frac{1-\delta_N}{2}n_N \equiv x_p n_N,\tag{11}$$

$$n_d = \frac{1+\delta_Q}{2}N_c n_Q \equiv x_d N_c n_Q,\tag{12}$$

$$n_u = \frac{1-\delta_Q}{2}N_c n_Q \equiv x_u N_c n_Q.\tag{13}$$

The u and d quark Fermi momenta are simply related to their densities as

$$k_{F_u}^3 = \frac{3\pi^2}{N_c}n_u = (1-\delta_Q)k_{F_Q}^3,\tag{14}$$

$$k_{F_d}^3 = \frac{3\pi^2}{N_c}n_d = (1+\delta_Q)k_{F_Q}^3,\tag{15}$$

since d and u quarks occupy their Fermi sphere, see Fig. 1.

The neutron and proton Fermi layers can be calculated from the difference of two Fermi spheres with different radii defined as,

$$n_n = \frac{1}{3\pi^2}\left(k_{F_n}^3 - k_{F_n^{\min}}^3\right),\ n_p = \frac{1}{3\pi^2}\left(k_{F_p}^3 - k_{F_p^{\min}}^3\right),\tag{16}$$

where $k_{F_n^{\min}}$ and $k_{F_p^{\min}}$ are the lower bound of the nucleon shell, see Fig. 1. Injecting Eq. (4) into $n_i = x_i n_N$ ($i = n$, p) and identifying with Eqs. (16), we obtain

$$k_{F_n}^3 = (1+\delta_N)k_{F_N}^3,\qquad k_{F_p}^3 = (1-\delta_N)k_{F_N}^3,\tag{17}$$

as well as

$$k_{F_n^{\min}}^3 = (1+\delta_N)\left(N_c k_{F_Q}\right)^3,\tag{18}$$

$$k_{F_p^{\min}}^3 = (1-\delta_N)\left(N_c k_{F_Q}\right)^3.\tag{19}$$

Note that $k_{F_n^{\min}}$ and $k_{F_p^{\min}}$ can be re-expressed as $k_{F_i}^{\min} = (2x_i)^{1/3} N_c k_{F_Q} = N_c (3\pi^2 x_i n_Q)^{1/3}$, for $i = n, p$.

At low densities, in the absence of quarks $k_{F_Q} = 0$, so neutrons and protons occupy entirely their Fermi spheres with radii given by Eqs. (17). It is interesting to note that Eqs. (17) are identical in the presence or the absence of quarks.

Now that the Fermi spheres and the Fermi shells for n, p, u and d particles are well defined, all thermodynamical quantities can be determined, e.g. the energy of the ground state, the pressure, the chemical potentials, or the sound speed.

C. Energy density and derivatives

The energy density of quarkyonic matter is given by

$$\rho_B = \rho_N + \rho_Q \,, \tag{20}$$

where the nucleon and quark terms are given by:

$$\rho_N = 2 \sum_{i=n,p} \int_{k_{F_i}^{\min}}^{k_{F_i}} \frac{d^3k}{(2\pi)^3} \sqrt{k^2 + M_N^2} + V_N(n_n, n_p)\,, \tag{21}$$

$$\rho_Q = 2 \sum_{q=u,d} N_c \int_0^{k_{F_q}} \frac{d^3k}{(2\pi)^3} \sqrt{k^2 + M_Q^2}\,, \tag{22}$$

with the nuclear residual interaction given by the meta-model [19],

$$V_N(n_n, n_p) = \sum_\alpha \frac{1}{\alpha!} c_\alpha(\delta_N) x^\alpha u_\alpha(x)\,, \tag{23}$$

where $x = (n_N - n_{\text{sat}})/(3n_{\text{sat}})$, $c_\alpha(\delta_N) = c_{\text{sat},\alpha} + c_{\text{sym},\alpha} \delta_N^2$ and $u_\alpha(x) = 1 - (-3x)^{N+1-\alpha} \exp(-b\, n_N/n_{\text{sat}})$. The coefficients $c_{\text{sat},\alpha}$ and $c_{\text{sym},\alpha}$ are related to the empirical parameters, e.g. $E_{\text{sat}} \approx -16$ MeV, $n_{\text{sat}} \approx 0.16$ fm^{-3} and $K_{\text{sat}} \approx 230$ MeV in nuclear matter, considering the relativistic extension of the meta-model (for the kinetic term only) [33]. The present calculation is based on the nucleon Skyrme interaction SLy4, on which the meta-model is adjusted. We consider the parameters given in table I.

The binding energy density ϵ_B is defined as

$$\epsilon_B(k_{F_N}, \delta_N) = \rho_B(k_{F_N}, \delta_N) - M_N n_B\,, \tag{24}$$

and the binding energy per baryon number is

$$e_B(k_{F_N}, \delta_N) = \epsilon_B(k_{F_N}, \delta_N)/n_B\,. \tag{25}$$

The other quantities as the chemical potentials, pressure and sound velocities are computed using the usual definitions, see Ref. [19, 34] for more details.

D. Results

In this section we compare a pure nucleon model for matter properties against quarkyonic models constructed on top of the same nucleon model. The choice of SLy4 is influenced by the fact that this pure nucleon model reproduces most of the recent observational data, such as the tidal deformability from GW170817 or the NICER x-ray observation of PSR J0030+0451. We then explore the influence of the quarkyonic model parameters Λ_{Qyc} and κ_{Qyc}.

The neutron chemical potential μ_n, the energy per particle E_B/A, the baryon pressure P_B and baryon sound speed $(v_{s,B}/c)^2$ are shown in Fig. 2 for SM (solid lines, $\delta_N = 0$), AM (dashed lines, $\delta_N = 0.5$) and NM (dotted lines, $\delta_N = 1$). The quarkyonic model parameters are fixed to be $\Lambda_{\text{Qyc}} = 250$ MeV and $\kappa_{\text{Qyc}} = 0.3$. The predictions for the quarkyonic phase (green lines) are confronted to the ones for the pure nucleon phase (magenta lines). The model predictions are stopped when causality is violated. The sound velocity in quarkyonic matter has a peak at around $n_B \approx 0.4$ fm^{-3}, as shown in Ref. [1] for SM and NM, and confirmed here for AM. The position of the peak is almost independent of the isospin asymmetry, but the peak is a bit more pronounced in NM compared to SM. For the chosen parameters, the sound speed predicted by the quarkyonic model at high density reaches a value close to the conformal limit, i.e. 1/3. The bump in the sound speed density profile present in quarkyonic matter impacts the pressure, the chemical potential and the binding energy. These thermodynamical quantities are strongly increased for densities where the sound speed is maximal, and they are softer at higher densities. The softening is such that the pressure of quarkyonic matter crosses the pure nucleon one at high density, see Fig. 2. The softening of the EoS is also predicted by usual construction of first order phase transitions from nucleon to quark matter, and the interesting feature of the quarkyonic model is the stiffening of the EoS at low densities, where it really matters for NS, before the softening at high density. The region of importance for NS properties coincides mostly with the densities where the pressure is stiff. This is the reason why this model is of particular interest for the phenomenology of compact stars.

The increase of the chemical potential in the crossover region can also be explained from the behavior of the nucleon Fermi momentum, which can be traced down from Eq. (4) and re-written as,

$$k_{F_N}^3 = \frac{3\pi^2}{2} \left[n_N + N_c^3 n_Q \right]\,, \tag{26}$$

showing that the quark contribution to the nucleon Fermi momentum is strongly enhanced by the factor N_c^3. As the density increases however, the quark component of matter becomes more and more dominant and the softening actually occurs.

The conclusion of this first set of results is that the generic features of the quarkyonic model predicted by McLerran and Reddy [1] are preserved in our extension of the quarkyonic model for AM, and we can predict similar features in NM with the same parameters as the one in SM. Our results are also in qualitative agreement with

Model	$E_{\rm sat}$	$E_{\rm sym}$	$n_{\rm sat}$	$L_{\rm sym}$	$K_{\rm sat}$	$K_{\rm sym}$	$Q_{\rm sat}$	$Q_{\rm sym}$	$Z_{\rm sat}$	$Z_{\rm sym}$	m^*/m	$\Delta m^*/m$	$b_{\rm sat}$
	MeV	MeV	fm^{-3}	MeV	MeV	MeV	MeV	MeV	MeV	MeV			
SLy4$_{\rm MM}^{\rm NR}$	-15.97	32.01	0.1595	46	230	-120	-225	400	-443	-690	0.69	-0.19	6.90
SLy4$_{\rm MM}^{\rm RL}$	-15.97	32.01	0.1595	46	230	-120	-225	400	-443	-690	1.0	0.0	6.90

TABLE I: Parameters of the SLy4 meta-model used in the non-relativistic (NR) case for the description of nuclear matter and in the relativistic case (RL), where only relativistic kinematic is considered, for the quarkyonic matter.
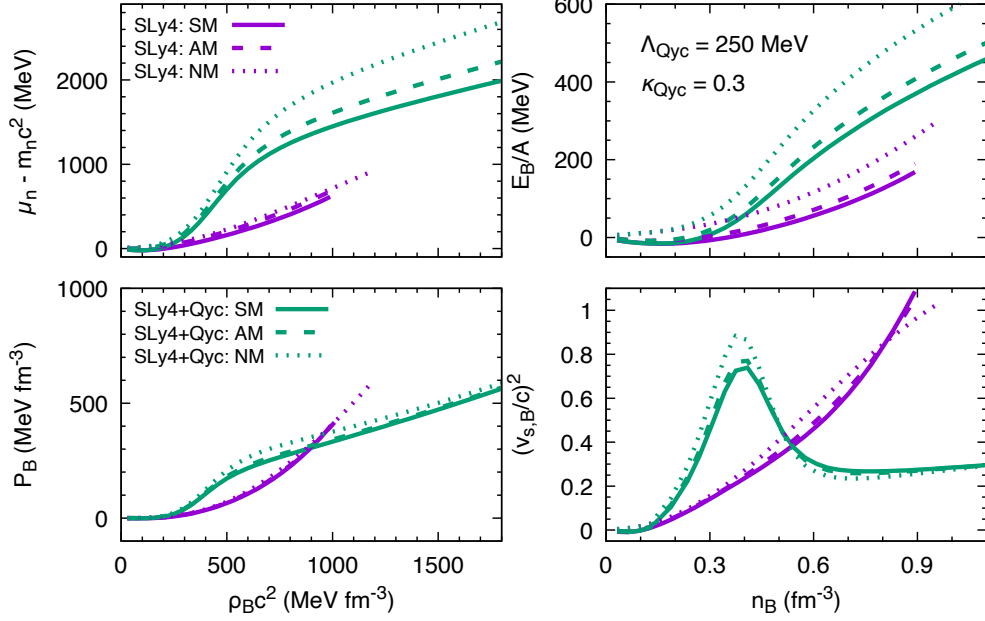
FIG. 2: Baryon chemical potential μ_B, energy per particle E_B/A, pressure P_B and sound speed $(v_{s,B}/c)^2$ in symmetric (SM, $\delta_N = 0.0$), asymmetric (AM, $\delta_N = 0.5$), and neutron matter (NM, $\delta_N = 1.0$) for $\Lambda_{\rm Qyc} = 250$ MeV and $\kappa_{\rm Qyc} = 0.3$.

the ones found by Zhao and Lattimer [27] as well as Jeong McLerran and Sen [29] where different nuclear potential were used.

II. QUARKYONIC MODEL AT β-EQUILIBRIUM

We are now constructing the beta-equilibrium solutions, which describe the ground state of dense matter existing in the core of compact stars. In cold catalyzed NS, matter components are determined from the β-equilibrium equations,

$$\mu_n - \mu_p = \mu_e , \qquad (27)$$
$$\mu_e = \mu_\mu , \qquad (28)$$

and charge neutrality,

$$n_e + n_\mu + \frac{1}{3}n_d = n_p + \frac{2}{3}n_u . \qquad (29)$$

At fixed total density, these three equations allows the determination of three variables: the isospin asymmetry δ_N and the electron and muon densities, n_e and n_μ.

Note that the charge neutrality condition (29) in NM becomes $n_d = 2n_u$, which coincides with the relation between u and d quark Fermi momenta, $k_{Fd} = 2^{1/3}k_{Fu}$, imposed in NM in [1].

The particle fractions in dense matter are shown in Fig. 3 for the SLy4 nucleon model (magenta) and the quarkyonic model taking $\Lambda_{\rm Qyc} = 250$ MeV and $\kappa_{\rm Qyc} = 0.3$ (green). On the left panel of Fig. 3 are shown only the baryon contributions, n, p, d and u, while on the right panel, the contributions of the nucleons, quarks, electrons and muons are represented. In the crossover region, neutron and proton densities are reduced compare to the original nucleon model while the amount of quarks increases. In particular, we observe that the fraction of protons is reduced in the quarkyonic model such that it remains below the dURCA threshold ($\gtrsim 1/9\%$ in the presence of muons [28]).

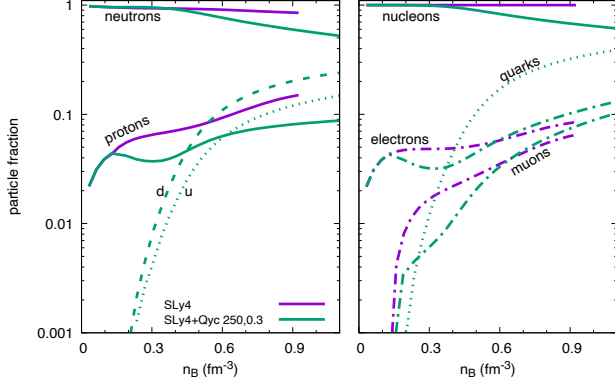In order to investigate the role of the parameters of

FIG. 3: Particle fractions for the SLy4 nucleon model and the quarkyonic model taking $\Lambda_{\text{Qyc}} = 250$ MeV and $\kappa_{\text{Qyc}} = 0.3$.
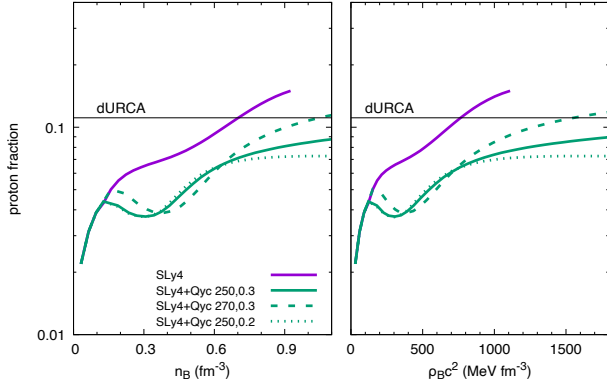

FIG. 4: Comparison of the proton fraction in the pure nucleon model with the prediction of the quarkyonic model for various sets of the parameters $(\Lambda_{\text{Qyc}}, \kappa_{\text{Qyc}})$: $(250, 0.3)$, $(270, 0.3)$ and $(250, 0.2)$. Left: function of the particle density in fm^{-3}, right: function of the energy density $\rho_B c^2$ in MeV fm^{-3}.

the quarkyonic model on the proton fraction, we show in Fig. 4 a comparison for different choices for the parameters $(\Lambda_{\text{Qyc}}, \kappa_{\text{Qyc}})$: $(250, 0.3)$, $(270, 0.3)$ and $(250, 0.2)$. Increasing Λ_{Qyc} from 250 MeV to 270 MeV induces an increase of the proton fraction at high density, which passes the dURCA threshold, but at higher density. In terms of energy density $\rho_B c^2$, right panel in Fig. 4, the dURCA threshold is pushed even higher, since the quarkyonic model predicts larger energy densities than the pure nucleon one.

Finally, the thermodynamical properties of quarkyonic matter at β-equilibrium are shown in Fig. 5: the neutron chemical potential μ_n, the total energy per particle E_{tot}/A, the equation of state $P(\rho_B c^2)$ and the total sound speed. The effect of varying the parameters of the quarkyonic matter is also shown. The largest impact is observed when the parameter Λ_{Qyc} in increased from

250 MeV to 270 MeV. Increasing Λ_{Qyc} has the effect of pushing the onset of the first quarks at higher density, as it can also be observed in Fig. 5. As a consequence, increasing Λ_{Qyc} makes quarkyonic matter more and more repulsive, except at low density where the larger Λ_{Qyc} the softer the EoS, as discussed previously. The effect of changing κ_{Qyc} is smaller. It was tuned in the original paper by McLerran and Reddy [1] to the conformal limit for the sound speed.

III. QUARKYONIC STARS

The structure of non-rotating neutron stars is provided by the solution of the spherical hydrostatic equations in general relativity, also named the Tolmann-Oppenheimer-Volkof equations [35],

$$\frac{dm(r)}{dr} = 4\pi r^2 \rho(r), \tag{30}$$

$$\frac{dP(r)}{dr} = -\rho(r)c^2 \left(1 + \frac{P(r)}{\rho(r)c^2}\right)\frac{d\Phi(r)}{dr},$$

$$\frac{d\Phi(r)}{dr} = \frac{Gm(r)}{c^2 r^2}\left(1 + \frac{4\pi P(r)r^3}{m(r)c^2}\right)\left(1 - \frac{2Gm(r)}{rc^2}\right)^{-1},$$

where G is the gravitational constant, c the speed of light, $P(r)$ the total pressure, $m(r)$ the enclosed mass, $\rho(r) = \rho_B(r)$ is the total mass-energy density and $\Phi(r)$ the gravitational field. P and ρ have contributions from both the baryons (P_B, ρ_B) and the leptons (P_L, ρ_L).

The four variables (m, ρ, P, Φ) are obtained from the solution of the three TOV equations (30) and the EoS for the quarkyonic matter. In the present calculation, a crust EoS is smoothly connected to the core EoS as described in Ref. [34]. The tidal deformability Λ_{GW} induced by an external quadrupole field is expressed in terms of the Love number k_2 as $\Lambda_{GW} = 2k_2/(3C^5)$, where the compactness is $C = GM/(Rc^2)$, and k_2 is calculated from the pulsation equation at the surface of NS [11, 12],

$$k_2 = \frac{8C^5}{5}(1-2C)^2(2-y_R+2C(y_R-1))$$
$$\times\Big(2C(6-3y_R+3C(5y_R-8))$$
$$+4C^3\left(13-11y_R+C(3y_R-2)+2C^2(1+y_R)\right)$$
$$+3(1-2C)^2(2-y_R+2C(y_R-1))\ln(1-2C)\Big)^{-1}, \tag{31}$$

where y_R is the value of the y function at radius R, $y_R = y(r = R)$, and $y(r)$ is the solution of the following differential equation,

$$r\frac{dy}{dr} + y^2 + yF(r) + r^2 Q(r) = 0, \tag{32}$$
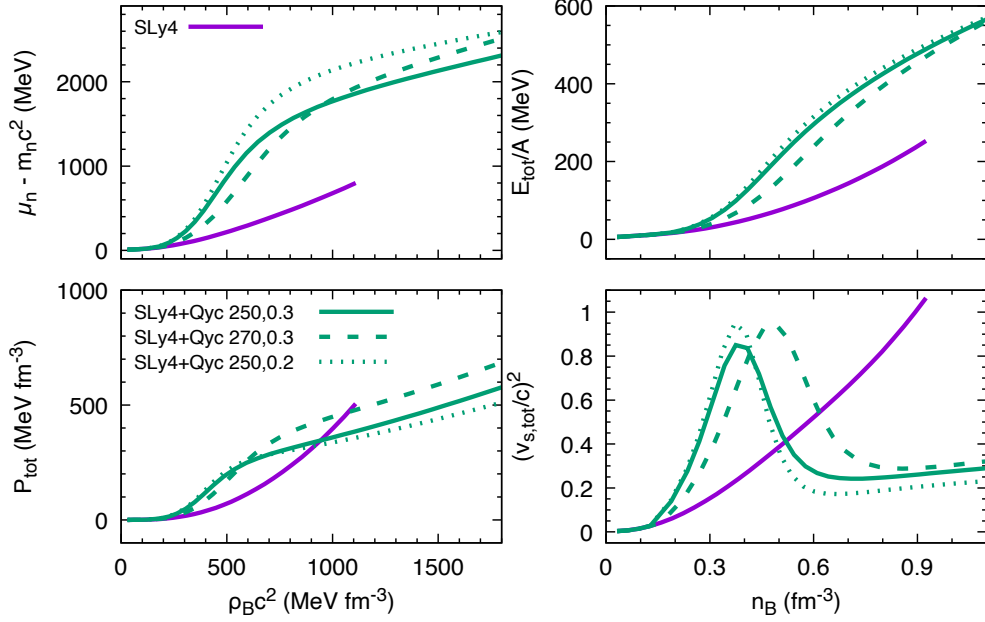
with the boundary condition $y(0) = 2$ and the functions

FIG. 5: Neutron chemical potential μ_n, total energy per particle E_{tot}/A, total pressure P_{tot} and total sound speed $(v_{s,tot}/c)^2$ at β-equilibrium for the parameters $(\Lambda_{\mathrm{Qyc}}, \kappa_{\mathrm{Qyc}})$, same choice as in Fig. 4.

$F(r)$ and $Q(r)$ defined as,

$$F(r) = \frac{1 - 4\pi r^2 G[\rho(r) - P(r)]/c^4}{1 - 2M(r)G/(rc^2)}, \qquad (33)$$

$$r^2 Q(r) = \frac{4\pi r^2 G}{c^4} \left(5\rho(r) + 9P(r) + \frac{\partial \rho(r)}{\partial P(r)}[\rho(r) + P(r)] \right)$$
$$\times \left(1 - 2M(r)G/(rc^2) \right)^{-1} - 6 \left(1 - 2M(r)G/(rc^2) \right)^{-1}$$
$$- \frac{4G^2}{r^2 c^8} \left(M(r)c^2 + 4\pi r^3 P(r) \right)^2 \left(1 - 2M(r)G/(rc^2) \right)^{-2}. \qquad (34)$$

The NS moment of inertia is obtained from the slow rotation approximation [36, 37] as

$$I = \frac{8\pi}{3} \int_0^R dr \, r^4 \rho(r) \left(1 + \frac{P}{\rho(c)c^2} \right) \frac{\bar{\omega}}{\Omega} e^{\lambda - \Phi}, \qquad (35)$$

where $\bar{\omega}$ is the local spin frequency, which represents the general relativistic correction to the asymptotic angular momentum Ω and λ is defined as $\exp(-2\lambda) = 1 - Gm/(rc^2)$.

As usual, for a given EoS the family of solutions is parameterized by the central density or pressure or enthalpy. The EoS are characterized by their evolution in the mass-radius diagram, where both masses and radii of compact stars could in principle be measured, as discussed in our introduction, see also Ref. [38].

We show in Fig. 6 the predictions for the mass M, radius R, tidal deformability Λ_{GW}, central density n_c, binding energy E_{bind} and moment of inertia I associated to various quarkyonic EoS with $(\Lambda_{\mathrm{Qyc}}, \kappa_{\mathrm{Qyc}})$: $(250, 0.3)$,

$(270, 0.3)$ and $(250, 0.2)$ (green lines). These predictions are confronted to the ones for a nucleon EoS (solid magenta line).

The impact of quarkyonic matter on the mass-radius relation is huge, as already noticed in Refs. [1, 29]. While the maximum mass for SLy4 is reached at 2.03 $M_\odot$, the quarkyonic stars almost reach 3 $M_\odot$. These is also a large impact on the radius: the 1.4 $M_\odot$ radius $R_{1.4}$ of the pure nucleon model is about 11.5 km, while it is pushed up to 13-14 km in the quarkyonic model. Quarkyonic stars can therefore be much more massive than pure nucleon ones, and are also bigger in size. Quarkyonic stars have also different tidal deformabilities Λ_{GW} compared to the pure nucleon case. For the same mass, the quarkyonic stars have larger Λ_{GW}, and at fixed Λ_{GW}, they have larger radii. At a fixed central density (in fm^{-3}), quarkyonic stars are much more massive than the pure nucleon model we considered. This is an effect of the repulsion observed for the pressure in Fig. 5. For the same mass, quarkyonic stars have a slightly lower E_{bind} compared to the associated nucleonic star, they however have a larger moment of inertia.

One can estimate the influence of the parameters Λ_{Qyc} and κ_{Qyc}. As observed in previous figures, the parameter κ_{Qyc} is almost not influential at all, while Λ_{Qyc} is much more critical. By increasing Λ_{Qyc}, the realization of quarkyonic matter is pushed up and the EoS get closer to the pure nucleon case. The quarkyonic star therefore also get a bit closer to the neutron star as Λ_{Qyc} increases. The journey in the mass-radius diagram is therefore very much controlled by the parameter Λ_{Qyc}. By decreasing Λ_{Qyc} the quarkyonic star gets bigger and bigger com-
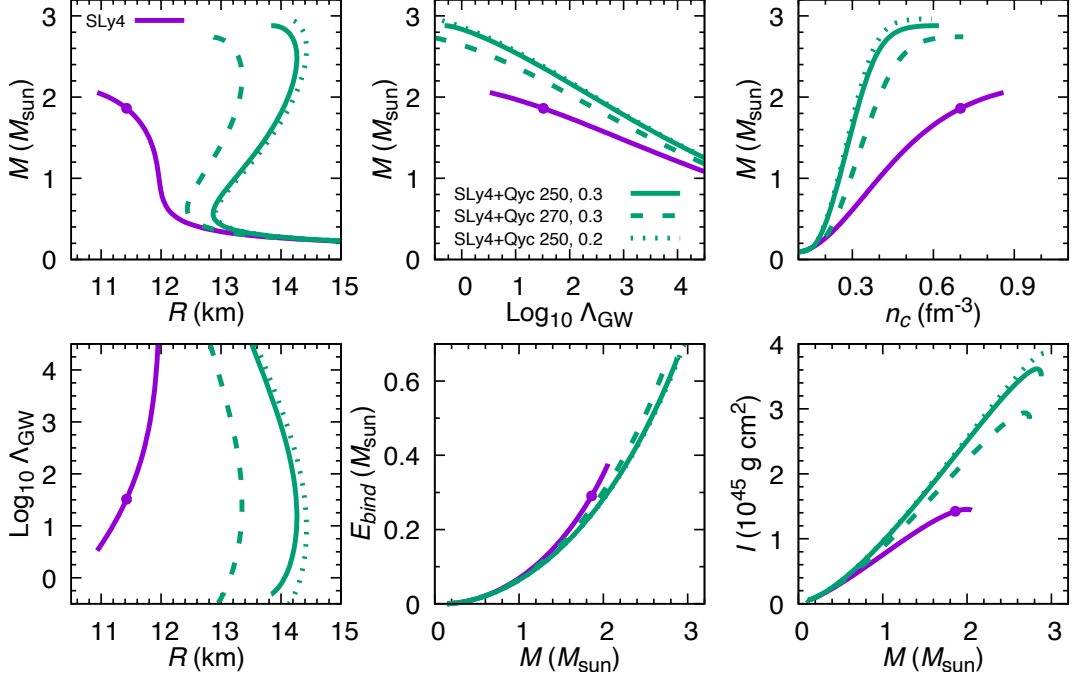
9

FIG. 6: Neutron star properties (mass M, radius R, tidal deformability Λ_{GW}, central density n_c, binding energy $E_{bind} = M_b - M$, where M_b is the baryon mass, and the moment of inertia I) for quarkyonic matter with Λ_{Qyc} and κ_{Qyc} fixed as in Fig. 4 (green curves) and nucleon matter (solid magenta curve).

pared to the NS, as well as it gets more and more massive. In the future, the observation of several points in mass and radius, e.g. from NICER observations, will thus be very useful for the determination of the parameter Λ_{Qyc}.

Finally we discuss the dURCA threshold, represented in the curves by the solid circle. Only the pure nucleon case reaches the dURCA threshold, and it happens close to 2 $M_\odot$. Even the quarkyonic model with (Λ_{Qyc}, κ_{Qyc})=(270, 0.3), which satisfies the dURCA condition at high density, see Fig. 4, reaches the unstable branch before it gets to the dURCA density. It is thus more difficult to reach the dURCA condition with quarkyonic stars. The same conclusion was also obtained by Zhao and Lattimer [27] with their version of quarkyonic matter.

We show in Fig. 7 the NS compactness defined as $(M/M_\odot)/(R/\text{km})$, where R is expressed in km, function of the mass (left panel) and of the radius (right panel). The compactness of the isolated NS RX J0720.4-3135 has been extracted from observations and estimated to be 0.105±0.002 [39]. Reporting this value in the left panel of Fig. 7 we observe that the nucleonic EoS SLy4 suggests that the mass of the pulsar is 1.25 $M_\odot$, compatible with observed masses but close to their lower limit [40], while the quarkyonic model suggest higher masses, up to 1.43 $M_\odot$, which is compatible with the canonical NS mass. Note that a Bayesian exploration of nucleonic models has predicted a centroid of about 1.33 $M_\odot$ [34].
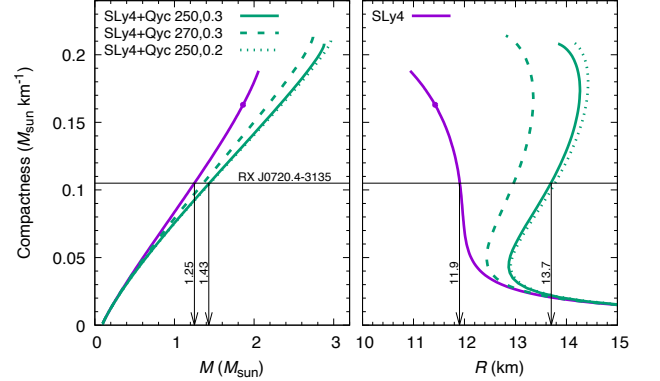

FIG. 7: Compactness $(M/M_\odot)/(R/\text{km})$ as function of the mass $M/M_\odot$ (left) and radius (right) for various sets of the parameters Λ_{Qyc} and κ_{Qyc} fixed to be as in Fig. 4.

This value is slightly larger than the one suggested by SLy4 EoS, but is still lower that the canonical mass. On the right panel of Fig. 7 the radii associated to the observed compactness are also reported. While the SLy4 EoS favors 11.9 km, the quarkyonic stars point towards larger radii, up to 13.6 km in the upper case. So we conclude that for a fixed value of the compactness, Fig. 7 shows that quarkyonic stars have larger masses and radii
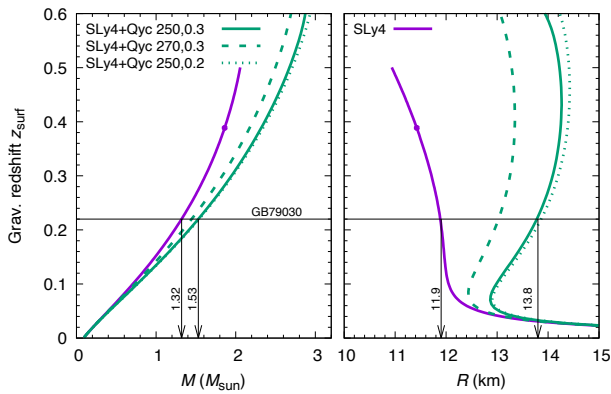
FIG. 8: Gravitational redshift z_{surf} as function of the mass $M/M_\odot$ (left) and radius (right) for various sets of the parameters Λ_{Qyc} and κ_{Qyc} fixed to be as in Fig. 4.

FIG. 9: Mass-radius relation for SLy4-soft nuclear interaction and for the quarkyonic model with various sets of the parameters Λ_{Qyc} and κ_{Qyc} fixed to be as in Fig. 4.

than NS.

The gravitational redshift z_{surf} associated to the radial emission of photons from the surface, which is detected by a distant observer is defined as $z_{surf} = \left(1 - 2GM/(Rc^2)\right)^{-1/2} - 1$. In Fig. 8 we show z_{surf} versus the stellar mass (left panel) and versus the stellar radius (right panel). The emission line feature of the gamma ray burst GB790305, assumed to originate from the e^-e^+ annihilation (observed peak at 430 keV, line width 150±20 keV), and assuming thermal nature of line broadening and taking due account of the thermal blueshift, leads to the observational constraint $z_{surf}^{GB790305} = 0.22$ [41, 42], which is reported in Fig. 8. We also deduce from this observational data that SLy4 would favor typical masses of the order of 1.32 $M_\odot$, low masses, while the quarkyonic star built on the same nucleonic star would point towards 1.53 $M_\odot$, closer to the canonical NS mass. The radius of extracted from SLy4 would be 11.9 km, while quarkyonic star would point towards larger radii, up to about 13.8 km.

Finally, we construct the quarkyonic model on top of a nucleonic model which does not reach the observation constraint of about $2M_\odot$. To do so, we reduce the value of Z_{sym} from the SLy4 nucleonic model by 300 MeV, see table I. The nucleonic model is shown in Fig. 9 under the label SLy4-soft (solid magenta line) while the quarkyonic models are shown for the same three cases as before. With this example, we show that the crossover transition to quark matter, as described by the quarkyonic approach, can bring enough repulsion to reach large maximum mass, even if the model for the nucleonic part cannot satisfy the observed requirement that the maximal mass of NS should be above about $2M_\odot$.
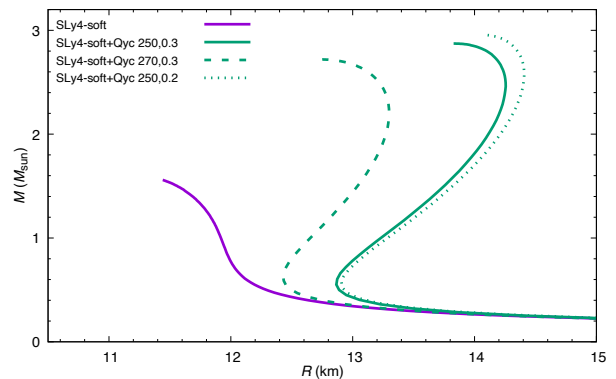
IV. CONCLUSIONS

We have proposed an extension of the original quarkyonic model from Ref. [1] to AM, where the original quarkyonic model for SM is recovered as a limit. Our extension assumes (i) that the description of the quark Fermi see and nucleon shell is globally isoscalar and (ii) that the isospin-flavor asymmetry in the quark and nucleon phases is fixed. These assumptions root into the concept of the quarkyonic model where nucleons result from the strong confining force, which strength is large close to the Fermi level. The assumption (i) allows us to smoothly connect to the quarkyonic model in SM, and suggests a description of NM quite comparable – at least qualitatively – to the original one suggested by McLerran and Reddy [1]. By fixing the isospin/flavor asymmetry in the nucleon and quark phases, assumption (ii), the properties of isospin asymmetric quarkyonic matter can be entirely determined from the nucleon Fermi momentum k_{F_N} and the isospin asymmetry δ_N.

NS matter at β-equilibrium is then been calculated and it provides qualitatively similar results as in the original model [1]. It is also in agreement with other extensions in asymmetric matter [27, 29], while being based on different assumptions. In our model, quarkyonic stars are larger and heavier than the associated NS, and the parameter Λ_{Qyc} is playing a dominant role in changing the radius and the mass of quarkyonic stars. This result is valid even if the nucleonic component is soft, e.g. too soft to reach $2M_\odot$. The proton fraction at β-equilibrium is found to be reduced in the quarkyonic matter, compared to the related pure nucleonic phase, which potentially quench fast cooling – based on dURCA process – in massive compact stars. The confrontation to a set of masses and radii, potentially obtained in future observations like NICER or gravitational wave detections of in-spiral binary NS, will potentially constrain Λ_{Qyc}, as

well as cooling scenarios.

In the future, we aim at incorporating the quarkyonic model in systematical comparisons to observational data in order to better understand the properties of dense matter. Extension of the present model to finite temperature is also on our map for the near future, as well as improving the isospin/flavor asymmetry relation. Also, adding chiral symmetry consideration in the quarkyonic model, taking into account the two most striking features of QCD, will certainly be an interesting extension to study.

[1] L. McLerran and S. Reddy, Phys. Rev. Lett. 122, 122701 (2019).
[2] The Physics and Astrophysics of Neutron Stars, L. Rezzolla et al. Editors, Springer International Publishing (2018).
[3] P. Haensel, A. Y. Potekhin, and D. G. Yakovlev, Neutron Stars I (Springer, Berlin, 2007).
[4] B. P. Abbott et al. (LIGO Scientific Collaboration and Virgo Collaboration), Phys. Rev. Lett. 119, 161101 (2017).
[5] J. Antoniadis, P.C.C. Freire, N. Wex et al., Science 340, 448 (2013).
[6] F. Özel and P. Freire, Annu. Rev. Astron. Astrophys. 54, 401 (2016).
[7] E. Fonseca, T.T. Pennucci, J.A. Ellis, et al., Astro. J 832, 167 (2016).
[8] M. Linares, T. Shahbaz, and J. Casares, Astrophys. J. 859, 54 (2018).
[9] H. T. Cromartie et al., Nat. Astron. 4, 72 (2020).
[10] Z. Arzoumanian, A. Brazier, S. Burke-Spolaor et al., Astro. J. SS 235, 37 (2018).
[11] T. Hinderer, Astrophys. J. 677, 1216 (2008).
[12] É.É. Flanagan and T. Hinderer, Phys. Rev. D 77, 021502 (2008).
[13] M.W. Coughlin, T. Dietrich, B. Margalit, and B.D. Metzger, MNRAS 489, L91 (2019).
[14] S. Guillot, M. Servillat, N.A. Webb, & R.E. Rutledge, Astrophys. J 772, 7 (2013).
[15] A.W. Steiner, C.O. Heinke, S. Bogdanov, et al., MNRAS 476, 421 (2018).
[16] N. Baillot d'Etivaux, S. Guillot, J. Margueron, N. A. Webb, M. Catelan, A. Reisenegger, Astrophys. J. 887, 48 (2019).
[17] C. A. Raithel, F. Özel and D. Psaltis, Astrophys. J. 831, 44 (2016).
[18] K. Gendreau and Z. Arzoumanian, Nat. Astron. 1, 895 (2017).
[19] J. Margueron, R. Casali Hoffmann, F. Gulminelli, Phys. Rev. C 97, 025805 (2018).
[20] L. McLerran and R.D. Pisarski, Nucl. Phys. A 796, 83 (2007).

[21] K. Fukushima, and T. Kojo, Astrophys. Journ. 817, 180 (2016).
[22] N. Kovenky and A. Schmitt, Journ. High En. Phys. 09, 112 (2020).
[23] J. Zdunik and P. Haensel, Astron. & Astrophys.551, A61 (2013).
[24] M.G. Alford, S. Han, Phys. Rev. D 88, 083013 (2013); M.G. Alford, G.F. Burgio, S. Han, G. Taranto, and D. Zappalà, Phys. Rev. D 92, 083002 (2015).
[25] P. Bedaque and A.W. Steiner, Phys. Rev. Lett. 114, 031103 (2015).
[26] I. Tews, J. Carlson, S. Gandolfi, and S. Reddy, Astrophys. J. 860, 149 (2018).
[27] T. Zhao and J. L. Lattimer, Phys. Rev. D 102, 023021 (2020).
[28] J. L. Lattimer, C. Pethick, M. Prakash, and P. Haensel, Phys. Rev. Lett. 66, 2701 (1991).
[29] K. S. Jeong, L. McLerran, and S. Sen, Phys. Rev. C 101, 035201 (2020).
[30] D. C. Duarte, S. Hernandez-Ortiz, and K. S. Jeong, Phys. Rev. C 102, 025203 (2020).
[31] D. C. Duarte, S. Hernandez-Ortiz, and K. S. Jeong, Phys. Rev. C 102, 065202 (2020).
[32] P. G. De Gennes, Superconductivity Of Metals And Alloys. Advanced Book Classics. Advanced Book Program, (Perseus Books, 1999).
[33] J. Margueron, unpublished.
[34] J. Margueron, R. Casali Hoffmann, F. Gulminelli, Phys. Rev. C 97, 025806 (2018).
[35] R. C. Tolman, Phys. Rev. 55, 364 (1939); J. R. Oppenheimer and G. M. Volkoff, Phys. Rev. 55, 374 (1939).
[36] J. B. Hartle and D. H. Sharp, Astrophys. J. 147, 317 (1967).
[37] I. A. Morrison, T.W. Baumgarte, S. L. Shapiro, and V. R. Pandharipande, Astrophys. J. 617, L135 (2004).
[38] A. Watts et al., PoS 215 (AASKA14), 043 (2015).
[39] V. Hambaryan, V. Suleimanov, F. Haberl et al., Astron. Astrophys. 601, A108 (2017).
[40] F. Özel and P. Freire, Ann. Rev. Astron. Astrophys. 54, 401 (2016).
[41] E. P. Mazets, S. V. Golenetskii, Yu. A. Guryan, and V. N. Ilyinskii, Astrophy. Space Science 84, 173 (1982).
[42] J. C. Higdon, and R. E. Lingenfelter, Ann. Rev. Astron. Astrophys. 28, 401 (1990).